

# Materials Design using Correlated Oxides: Optical Properties of Vanadium Dioxide

Jan M. Tomczak<sup>1,2</sup> and Silke Biermann<sup>3,2</sup>

<sup>1</sup>*Research Institute for Computational Sciences, AIST, Tsukuba, 305-8568 Japan*

<sup>2</sup>*Japan Science and Technology Agency, CREST*

<sup>3</sup>*Centre de Physique Théorique, Ecole Polytechnique, CNRS, 91128 Palaiseau Cedex, France*

Materials with strong electronic Coulomb interactions play an increasing role in modern materials applications. “Thermochromic” systems, which exhibit thermally induced changes in their optical response, provide a particularly interesting case. The optical switching associated with the metal-insulator transition of vanadium dioxide ( $\text{VO}_2$ ), for example, has been proposed for use in “intelligent” windows, which selectively filter radiative heat in hot weather conditions. In this work, we develop the theoretical tools for describing such a behavior. Using a novel scheme for the calculation of the optical conductivity of correlated materials, we obtain quantitative agreement with experiments for both phases of  $\text{VO}_2$ . On the example of an optimized energy-saving window setup, we further demonstrate that theoretical materials design has now come into reach, even for the particularly challenging class of correlated electron systems.

PACS numbers:

The concerted behavior of electrons in materials with strong electronic Coulomb interactions causes an extreme sensitivity to external stimuli, such as temperature, pressure or external fields. Heating insulating  $\text{SmNiO}_3$  beyond 400 K or applying a pressure of just a few kbar to the Mott insulator  $(\text{V}_{1-x}\text{Cr}_x)_2\text{O}_3$  ( $x=0.01$ ), e.g., make the materials undergo transitions to metallic states [1]. This tuneability of fundamental properties is both a harbinger for diverse technological applications and a challenge for a theoretical description. Indeed, many materials used in modern applications fall in this class of strongly correlated materials where electron-electron interactions profoundly modify (if not invalidate) a pure band picture. State-of-the-art first principles methods, such as density functional theory, are then no longer sufficient to predict physical properties of these compounds.

An increasing role is nowadays played by artificial structures, ranging from spintronic multi-layers [2, 3] to functional surfaces, where appropriate coatings e.g. provide a self-cleaning mechanism [4]. However, the huge freedom in the design, which concerns not only the chemical composition, the doping and the growth conditions, but also the geometry of the setup (e.g. the layer thicknesses), makes the search for devices with specific electronic properties a tedious task. Ideally, the quest for promising materials and setups should therefore be seconded by theoretical predictions. Yet, the abundance of fruitful experimental work on tailoring e.g. materials with specific optical absorption profiles is met with only scarce contributions from theoretical investigations [5].

Here, we demonstrate that even for the particularly challenging class of correlated materials a *quantitative* description, and thus predictions, are possible. We introduce a novel scheme for the calculation of optical properties, which can in principle be employed in conjunction with any electronic structure technique that uses localized basis functions. We shall demonstrate the

power of the approach within the framework of the combined density functional - dynamical mean field method “LDA+DMFT” [6], on the example of the optical conductivity of vanadium dioxide,  $\text{VO}_2$ . We further investigate  $\text{VO}_2$  based heterostructures and show that theoretical materials design of correlated material-derived devices is coming into reach.

Within dynamical mean field theory, emphasis is commonly put on *spectral* properties, and the evaluation of observables other than spectral functions is a rather new advancement in the realistic context. Yet, as explained above, it is the *response* behavior of correlated systems that is promising for applications. In this vein, recent pioneering work [7, 8, 9, 10, 11] has successfully described qualitative features of the optical response of several correlated materials. The calculation of absolute values in theoretical response functions – a prerequisite for quantitative theoretical materials design – has, however, turned out to be a formidable challenge. This is mainly due to the sensitivity of the obtained results on the accuracy of the transition matrix elements [12].

In the framework of linear response theory, and when neglecting vertex-corrections [16], the optical conductivity can be expressed as (for reviews see [12, 17])

$$\begin{aligned} \text{Re } \sigma^{\alpha\beta}(\omega) = & \frac{2\pi e^2 \hbar}{V} \sum_{\mathbf{k}} \int d\omega' \frac{f(\omega') - f(\omega' + \omega)}{\omega} \\ & \times \text{tr} \left\{ A_{\mathbf{k}}(\omega' + \omega) v_{\mathbf{k},\alpha} A_{\mathbf{k}}(\omega') v_{\mathbf{k},\beta} \right\} \end{aligned} \quad (1)$$

Correlation effects enter the calculation via the spectral functions  $A_{\mathbf{k}}(\omega)$ , while the Fermi velocities  $v_{\mathbf{k},\alpha} = \frac{1}{m} \langle \mathbf{kL}' | \mathcal{P}_\alpha | \mathbf{kL} \rangle$ , matrix elements of the momentum operator  $\mathcal{P}$ , which weight the different transitions, are determined by the band-structure. Both, spectral functions and velocities are matrices in the basis of localized orbitals, indexed by  $L = (n, l, m, \gamma)$ , with the usual quantum numbers  $(n, l, m)$ , while  $\gamma$  denotes the atoms in the

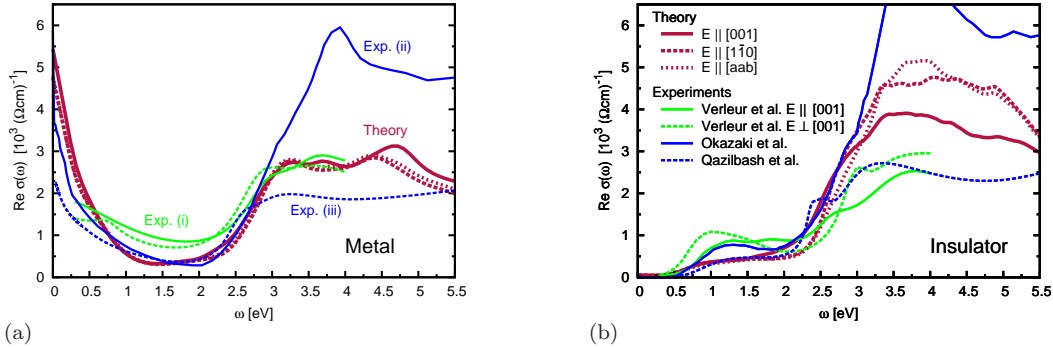


FIG. 1: Optical conductivity of (a) metallic, (b) insulating  $\text{VO}_2$  for polarizations  $E$ . Theory (red) ( $[\text{aab}]=[0.85\ 0.85\ 0.53]$ ), experimental data (i) single crystals [13] (green), (ii) thin film [14] (solid blue), (iii) polycrystalline film [15] (dashed blue).

unit cell :  $|\mathbf{k}L\rangle$  is the Fourier transform of the Wannier function  $\chi_{\mathbf{R}L}(\mathbf{r})$  localized at atom  $\gamma$  in the unit cell  $\mathbf{R}$ . The Fermi functions  $f(\omega)$  select the range of occupied and empty energies, respectively,  $V$  is the unit-cell volume,  $\alpha, \beta$  denote cartesian coordinates, and  $\text{Re } \sigma^{\alpha\beta}$  is the response in  $\alpha$ -direction for a light polarization  $E$  along  $\beta$ . Approaches such as LDA+DMFT [6] require the use of localized, Wannier-like, basis sets, rendering the evaluation of the full matrix element tedious. To this end, we developed a “generalized Peierls” approach that extends the formalism for lattice models (see the review [17]) to the realistic case of multi-atomic unit cells. We find that

$$v_{\mathbf{k},\alpha}^{L'L} = \frac{1}{\hbar} \left( \partial_{k_\alpha} \mathbf{H}_\mathbf{k}^{L'L} - i(\rho_{L'}^\alpha - \rho_L^\alpha) \mathbf{H}_\mathbf{k}^{L'L} \right) + \mathcal{F}_\mathbf{H} [\{\chi_{\mathbf{R}L}\}] \quad (2)$$

Here,  $\rho_L$  denotes the position of an atom within the unit-cell. The term in brackets, which is used in the actual calculations, we refer to as the “generalized Peierls” term : While the derivative term is the common Fermi velocity, the one proportional to the Hamiltonian originates from the generalization to realistic multi-atomic unit-cells. The correction term that recovers the full matrix element is denoted  $\mathcal{F}$  (for its explicit form see [12]). The latter reduces to purely atomic transitions,  $(\mathbf{R}, \gamma) = (\mathbf{R}', \gamma')$ , in the limit of strongly localized orbitals. In other words, the accuracy of the approach is controlled by the choice of basis functions. This generalized Peierls approach is thus expected to be a good approximation for systems with localized orbitals, such as the 3d or 4f orbitals in transition metal or lanthanide/actinide compounds. This expectation is indeed true as can be verified numerically [12]. From the optical conductivity, one can calculate the specular reflectivity and transmittance. Therewith, also the specular color of the material becomes accessible [34].

Our focus compound,  $\text{VO}_2$ , has attracted a lot of attention recently [18, 19]. It is among those materials in which correlation effects play a decisive role, to the extent that standard band-structure approaches fail to

capture even most basic experimental facts : In metallic  $\text{VO}_2$ , important incoherent spectral features witnessed by photoemission experiments are absent in band theory, and the metal-insulator transition at  $T_c=340$  K is missed altogether. For reviews see e.g. [12, 20] and references therein. Hence, any description of the thermochromic properties of this material must foot on an electronic structure approach that goes beyond band-theory and masters the many-body effects at work. Indeed, LDA+DMFT results for the spectral properties of  $\text{VO}_2$  agree well with experimental findings in both, the metallic [21, 22, 23] and the insulating phase [23]. Footing on the electronic structure calculation of Ref. [23] and our recent extension thereof [24, 25], we first employ our scheme to access optical properties of bulk  $\text{VO}_2$  both above and below its metal-insulator transition.

Fig. 1(a) shows our results for the optical conductivity of metallic  $\text{VO}_2$  as a function of frequency and in comparison with experimental data [13, 14, 15], see also [19]. As can be expected from the crystal structure [20], the optical response depends only weakly on the light polarization. The Drude-like metallic response is caused by transitions between narrow vanadium 3d excitations near the Fermi level, and thus affects only the low infra-red regime – a crucial observation as seen in the following. The shoulder at 1.75 eV still stems from intra-vanadium 3d contributions, while transitions involving oxygen 2p orbitals set in at 2 eV, henceforth constituting the major spectral weight up to the highest energies of the calculation. Also for insulating  $\text{VO}_2$ , see Fig. 1(b), the results are in good agreement with experiments. This time, a slight polarization dependence is seen in both, experiment and theory, owing to the change in crystal symmetry. Indeed, vanadium atoms pair up in the insulator to form dimers along the c-axis, leading to the formation of bonding/anti-bonding states for 3d orbitals [28]. Optical transitions between these orbitals result, in the corresponding energy range ( $\omega=1.5\text{--}2.5$  eV), in a higher amplitude of the conductivity for a light polarization par-

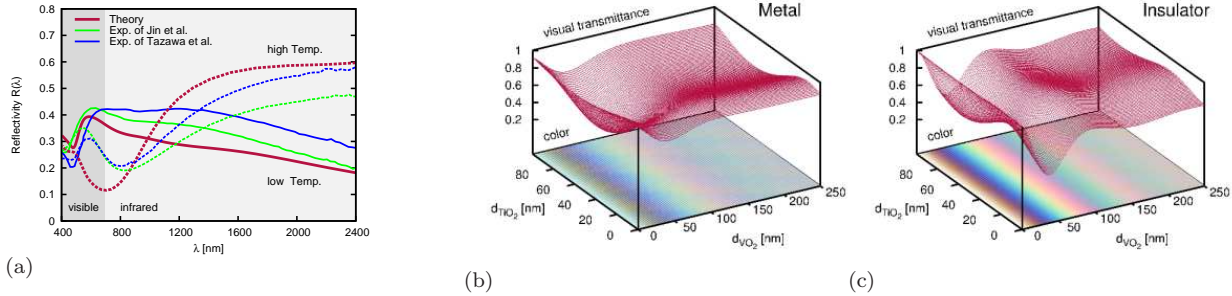


FIG. 2: Setups of an intelligent window. (a)  $\text{VO}_2$  on  $\text{SiO}_2$ . Reflectivity at high (dashed) and low temperatures (solid). Theory (red) : 60 nm  $\text{VO}_2$  on  $\text{SiO}_2$ . Experiments : 50 nm  $\text{VO}_2$  on  $\text{SiO}_2$  [26] (green), 50 nm  $\text{VO}_2$  on Pyrex glass [27] (blue). (b), (c) Setup with antireflexion coating :  $\text{TiO}_2$  /  $\text{VO}_2$  on  $\text{SiO}_2$ . Shown is the normalized visible transmittance (see text) an the corresponding color of the transmitted light for (b) high and (c) low temperature as a function of the layer thicknesses  $d_{\text{VO}_2}$  and  $d_{\text{TiO}_2}$ . All theoretical data for  $E \parallel [1\bar{1}0]$  polarization, and a 3mm  $\text{SiO}_2$  substrate.

allel to the c-axis than for other directions [12].

Having established the theoretical optical response of *bulk*  $\text{VO}_2$ , and thus verified that our scheme can *quantitatively* predict optical properties of correlated materials, we now investigate the possibilities of  $\text{VO}_2$ -based intelligent window coatings [29, 30]. The effect to be exploited can already be seen in the above bulk responses : The conductivities of both phases (Fig. 1(a), (b)) exhibit a close similarity in the range of visible light ( $\omega=1.7\text{--}3.0$  eV), whereas in the infra-red regime ( $\omega<1.7$  eV) a pronounced switching occurs across the transition. As a result, heat radiation can pass at low external temperatures, while its transmission is hindered above  $T_c$ . The insensitivity to temperature for visible light, in conjunction with the selectivity of the response to infrared radiation, is an essential feature of an intelligent window setup. Yet, for an applicable realization, other important requirements have to be met. First of all, the switching of the window has to occur at a relevant, that is ambient, temperature. Also, the total transmittance of  $\text{VO}_2$ -films in the visible range needs improvement [29], and the transmitted visible light should be uniform in order to provide a colorless vision. Experimentalists have addressed these issues and have proposed potential solutions [5] : Diverse dopings,  $M_xV_{1-x}O_2$ , were proved to influence  $T_c$ , with Tungsten ( $M=W$ ) being the most efficient : A doping of only 6% results in  $T_c \approx 20^\circ\text{C}$  [31]. However, this causes a deterioration of the infrared switching. Fluorine doping, on the other hand, improves on the switching properties, while also reducing  $T_c$  [32, 33]. An increase in the overall visible transmittance can also be achieved without modifying the intrinsic properties of the material itself, but by adding antireflexion coatings, for example  $\text{TiO}_2$  [26].

Here, we address the optical properties of window coatings from the theoretical perspective. In doing so, we assume that the specular response of  $\text{VO}_2$  layers is well-described by the optical properties of the bulk, and we

use geometrical optics to deduce the properties of layered structures. First, we consider the most simple of all setups, which consists of a single  $\text{VO}_2$ -layer (of thickness  $d_{\text{VO}_2}$ ) on a glass substrate [35]. Such a window has been experimentally investigated by Tazawa *et al.* [27] and Jin *et al.* [26]. In Fig. 2a we show their measured reflectivity data as a function of wavelength, in comparison with our theoretical results : At low temperatures (insulating  $\text{VO}_2$ ), the calculated reflectivity is in quantitative agreement with the experimental data. In the visible range ( $\lambda \approx 400\text{--}700$  nm), the reflectivity strongly depends on the wavelength. Therefore, the current window will filter certain wavelengths more than others, resulting in an illumination of a certain color – an obvious drawback. Moreover, the reflectivity in this region is rather elevated, causing poor global transmission. In the infrared regime ( $\lambda > 700$  nm) – and beyond – the reflectivity decreases, and radiation that causes greenhouse heating can pass the setup. At high temperatures, the infrared reflectivity switches to a rather elevated value, thus filtering heat radiation. The changes in the visible region are less pronounced, but still perceptible, and both, the degree of transparency and the color change through the transition. The current setup is thus not yet suited for applications.

We therefore now investigate a more complicated setup : An additional (rutile)  $\text{TiO}_2$ -coating is added on top of the  $\text{VO}_2$ -layer, with the objective of serving as an antireflexion filter [26]. With the thicknesses  $d_{\text{VO}_2}$  and  $d_{\text{TiO}_2}$ , the geometry of the current setup has two parameters that can be used to optimize the desired optical properties. Since, however, each variation of them requires the production of a new individual sample under comparable deposition conditions, along with a careful structural characterization in order to guarantee that differences in the optical behavior are genuine and not related to variations of the sample quality, the experimental expenditure is tremendous. This led Jin *et al.* [26] to

first estimate a highly transmitting setup by using tabulated refractive indices and to produce and measure only *one* such sample. Here, we shall use our theoretical results on VO<sub>2</sub> to not only optimize the geometry ( $d_{\text{TiO}_2}$ ,  $d_{\text{VO}_2}$ ) with respect to the total visible transmittance, but to also investigate the transmission color. Fig. 2 displays the normalized visible specular transmittance [36] for the window in its high (b) and low (c) temperature state, as a function of both film thicknesses. On the same graph the resulting transmission colors are shown. The evolution of the light interferences in the layers causes pronounced changes in both, the overall transmittance and the color. The coating of VO<sub>2</sub> globally degrades the transparency of the bare glass window. An increase of the TiO<sub>2</sub>-coating, on the other hand, has the potential to improve the total transmittance. This can be understood from the mechanism of common quarter-wave filters. The wavelength-dependence of the real-part of the TiO<sub>2</sub> refractive index,  $n_{\text{TiO}_2}(\lambda)$ , results in an optimal quarter-wave thickness,  $\delta_{\text{TiO}_2}(\lambda) = \lambda / (4n_{\text{TiO}_2}(\lambda))$ , which varies from blue to red light only slightly from  $\delta_{\text{TiO}_2}(\lambda) = 40$  to 60 nm. This and the fact that the imaginary part of the refractive index,  $k_{\text{TiO}_2}(\lambda)$ , is negligible for visible light explains why the color does not change significantly with  $d_{\text{TiO}_2}$ . While, as for TiO<sub>2</sub>, the variation of the real-part of the VO<sub>2</sub> refractive index yields a rather uniform ideal thickness  $\delta_{\text{VO}_2}(\lambda)$ , its imaginary part changes significantly (by a factor of 4) within the range of visible light. As a consequence, the color is very sensitive to VO<sub>2</sub>-deposition. At higher thickness  $d_{\text{VO}_2}$ , however, this dependence becomes smaller and the color lighter. Our theoretical transmittance profiles suggest relatively thick windows to yield good visual properties. Indeed, at low temperatures, Fig. 2(c), the local maximum that gives the thinnest window is located at  $(d_{\text{TiO}_2}, d_{\text{VO}_2}) \approx (40 \text{ nm}, 85 \text{ nm})$  within our calculation. However, this setup is still in the regime of important color oscillations. Given the uncertainties in industrial deposition techniques, it seems cumbersome to consistently stabilize colorless samples. From this point of view, a thicker VO<sub>2</sub>-film would be desirable. Indeed, while almost preserving the overall transmittance, a colorless window at low temperatures is realized for  $(d_{\text{TiO}_2}, d_{\text{VO}_2}) \approx (50 \text{ nm}, 220 \text{ nm})$ , or for  $(d_{\text{TiO}_2}, d_{\text{VO}_2}) = (\geq 100 \text{ nm}, 220 \text{ nm})$ . In the high temperature state, Fig. 2(b), the transmittance is globally lower than at low temperatures. Moreover, only  $(d_{\text{TiO}_2}, d_{\text{VO}_2}) = (\geq 100 \text{ nm}, 220 \text{ nm})$  yields a simultaneously high transmittance in *both* states of the window.

In conclusion, we have presented a novel scheme for the calculation of optical properties of correlated materials, and applied it to vanadium dioxide, VO<sub>2</sub>. We find the bulk optical conductivity of both phases in quantitative agreement with experiments, and further validate our approach by comparing the transmittance of a VO<sub>2</sub>-layer on SiO<sub>2</sub> to experimental data. Finally, we optimize the geometry of a multi-layer setup of an intelligent win-

dow, which uses the metal-insulator transition of VO<sub>2</sub> to reduce the effect of greenhouse heating. This work can be considered as a proof of principle of the feasibility of theoretical materials design, since our techniques can be applied to the general class of correlated materials.

We gratefully acknowledge discussions with T. Gacoin, G. Garry, A. Georges and L. Pourovskii. This work was supported by the Japan Science and Technology Agency (JST) under the CREST program, the French ANR under project CORRELMAT, and a computing grant by IDRIS Orsay under project number 081393.

---

- [1] M. Imada, A. Fujimori, and Y. Tokura, *Rev. Mod. Phys.* **70**, 1039 (1998).
- [2] M. N. Baibich, et al., *Phys. Rev. Lett.* **61**, 2472 (1988).
- [3] G. Binasch, et al., *Phys. Rev. B* **39**, 4828 (1989).
- [4] Y. Paz, et al., *J. Mater. Res.* **10**, 2842 (1995).
- [5] C. G. Granqvist, *Solar Energy Materials and Solar Cells* **91**, 1529 (2007).
- [6] G. Kotliar and D. Vollhardt, *Physics Today* **57**, 53 (2004).
- [7] N. Blümer, (PhD thesis, Universität Augsburg, 2002).
- [8] V. S. Oudovenko, et al., *Phys. Rev. B* **70**, 125112 (2004).
- [9] K. Haule, et al., *Phys. Rev. Lett.* **94**, 036401 (2005).
- [10] E. Pavarini, et al., *New Journal of Physics* **7**, 188 (2005).
- [11] L. Baldassarre, et al., *Phys. Rev. B* **77**, 113107 (2008).
- [12] J. M. Tomczak, (PhD thesis, Ecole Polytechnique, 2007).
- [13] H. W. Verleur, A. S. Barker, and C. N. Berglund, *Phys. Rev.* **172**, 788 (1968).
- [14] K. Okazaki, et al., *Phys. Rev. B* **73**, 165116 (2006).
- [15] M. M. Qazilbash, et al., *Phys. Rev. B* **74**, 205118 (2006).
- [16] A. Khurana, *Phys. Rev. Lett.* **64**, 1990 (1990).
- [17] A. J. Millis, in *Strong Interactions in Low Dimensions* (Physics and Chemistry of Materials with Low-Dimensional Structures, 2004), vol. 25, p. 195ff.
- [18] P. Baum, D.-S. Yang, and A. H. Zewail, *Science* **318**, 788 (2007).
- [19] M. M. Qazilbash, et al., *Science* **318**, 1750 (2007).
- [20] V. Eyert, *Ann. Phys. (Leipzig)* **11**, 650 (2002).
- [21] M. S. Laad, L. Craco, and E. Müller-Hartmann, *Europhys. Lett.* **69**, 984 (2005).
- [22] A. Liebsch, H. Ishida, and G. Bihlmayer, *Phys. Rev. B* **71**, 085109 (2005).
- [23] S. Biermann, et al., *Phys. Rev. Lett.* **94**, 026404 (2005).
- [24] J. M. Tomczak and S. Biermann, *J. Phys.: Cond. Matter* **19**, 365206 (2007).
- [25] J. M. Tomczak, F. Aryasetiawan, and S. Biermann (2007), submitted to *Phys. Rev. Lett.*, arXiv:0704.0902.
- [26] P. Jin, et al., *Appl. Phys. A* **77**, 455 (2003).
- [27] M. Tazawa, P. Jin, and S. Tanemura, *Appl. Opt.* **37**, 1858 (1998).
- [28] J. B. Goodenough, *J. Solid State Chem.* **3**, 490 (1971).
- [29] S. M. Babulanam, et al., *Sol. Energy Mater. Sol. Cells* **5**, 347 (1987).
- [30] C. G. Granqvist, *Thin Solid Films* **193-194**, 730 (1990).
- [31] M. A. Sobhan, et al., *Sol. Energy Mater. Sol. Cells* **44**, 451 (1996).
- [32] W. Burkhardt, et al., *Thin Solids Films* **402**, 226 (2002).
- [33] W. Burkhardt, et al., *Thin Solids Films* **345**, 229 (1999).

- [34] We employ the CIE 1964 conventions, along with the daylight illuminant D65, see e.g. K. Nassau. *The Physics and Chemistry of Color: The Fifteen Causes of Color*. (Wiley Series in Pure & Applied Optics, 2001).
- [35] We suppose quartz glass,  $\text{SiO}_2$ . All auxiliary refractive indices are taken from *Handbook of Optical Constants of Solids* by Edward D. Palik, Academic Press, 1985.
- [36]  $\int_{400\text{nm}}^{700\text{nm}} d\lambda S(\lambda)T(\lambda) / \int_{400\text{nm}}^{700\text{nm}} d\lambda S(\lambda)$ , with the spectrum

of the light source  $S(\lambda)$ , and the transmittance  $T = 1 - R$ ,  $R$  being the specular reflexion given by Fresnel's formulae. We thus neglect absorption due to inhomogeneities that lead to diffuse reflexion. This is justified for our applications to windows. Also,  $\text{VO}_2$  has a glossy appearance and hence a preponderant specular response.